Contributions of denitrification and mixing on the distribution of nitrous oxide in the North Pacific

Hiroaki Yamagishi,[1,2] Naohiro Yoshida,[1,2,3,4] Sakae Toyoda,[2,4] Brian N. Popp,[5] Marian B. Westley,[6] and Shuichi Watanabe[1,7]

Received 10 September 2004; revised 30 December 2004; accepted 12 January 2005; published 18 February 2005.

[1] We analyzed N_2O isotopomer ratios (distribution of isotopes within N_2O molecules) in the eastern tropical North Pacific. The N_2O isotopomer ratios indicate the contribution of denitrification in the oxygen minimum zone (OMZ, ~600 m in depth) in the western North Pacific, which is not consistent with the widely accepted nitrification hypothesis. Our models indicate that the N_2O yield per mole O_2 consumed ($dN_2O/-dO_2$) is 0.008 (0–0.015) nmol/μmol during remineralization and nitrification in the western North Pacific. Nitrification in aerobic deep waters is a minor source of oceanic N_2O, whereas the N_2O production in the OMZ is the dominant factor for the oceanic N_2O distribution. The denitrification in the OMZ is consistent with the correlation between ΔN_2O (level above atmospheric equilibrium) and AOU (apparent oxygen utilization), and the parallel ^{18}O-enrichment of N_2O and O_2 in the OMZ, which have been believed to support the nitrification hypothesis. **Citation:** Yamagishi, H., N. Yoshida, S. Toyoda, B. N. Popp, M. B. Westley, and S. Watanabe (2005), Contributions of denitrification and mixing on the distribution of nitrous oxide in the North Pacific, *Geophys. Res. Lett.*, *32*, L04603, doi:10.1029/2004GL021458.

1. Introduction

[2] Nitrous oxide (N_2O) is an important greenhouse gas and also plays a role in the stratospheric ozone chemistry. The ocean contributes approximately 20–30% of the total N_2O to the atmosphere [*Suntharalingam and Sarmiento*, 2000, and references therein]. Although microbial nitrification and denitrification can produce N_2O, there have been debates as to which process dominates the global oceanic N_2O source. Nitrification is supported by the correlation between ΔN_2O (level above atmospheric equilibrium) and AOU (apparent oxygen utilization) [*Yoshinari*, 1976], and the parallel ^{18}O-enrichment in N_2O and O_2 in the North Pacific [*Kim and Craig*, 1990]. However, the former evidence has recently been found to be ambiguous, because the slopes of the linear correlations between ΔN_2O and AOU are strongly influenced by mixing gradients and are unreliable gauges for the biological N_2O yield per mole O_2 consumed [*Nevison et al.*, 2003]. In contrast, denitrification is supported by the low ratio of N_2O to nitrate production during nitrification in ^{15}N-tracer experiments, which indicates that nitrification accounts for only one-tenth to one-fifth of the N_2O dissolved in the western North Pacific [*Yoshida et al.*, 1989]. Hence, the elucidation of the production processes and the contribution of mixing are essential for building a model for the oceanic N_2O cycle and for the prediction of future emission variations. Therefore, the objectives of this research are to resolve the contribution of each production process and global ocean circulation to the distribution of N_2O in the North Pacific, and to develop a reasonable explanation for the inconsistent evidence supporting the two opposing hypotheses.

[3] Recently, N_2O isotopomer ratios have shown promise in resolving the mechanism of N_2O production. The abundance ratios of $^{14}N^{15}N^{16}O$ and $^{15}N^{14}N^{16}O$ to $^{14}N^{14}N^{16}O$ are designated as $\delta^{15}N^{\alpha}$ and $\delta^{15}N^{\beta}$, respectively [*Toyoda and Yoshida*, 1999], and the difference between $\delta^{15}N^{\alpha}$ and $\delta^{15}N^{\beta}$ is defined as the site preference ($SP \equiv \delta^{15}N^{\alpha} - \delta^{15}N^{\beta}$) [*Yoshida and Toyoda*, 2000]. The high $\delta^{18}O$ and SP of N_2O in the oxygen minimum zone (OMZ) in the North Pacific relative to shallower depths are considered as indicators of the partial reduction of N_2O to N_2 by denitrification [*Popp et al.*, 2002] or the N_2O production by nitrification under substrate (NH_4^+)-limited conditions [*Toyoda et al.*, 2002]. We analyzed the isotopomer ratios of dissolved N_2O in the eastern tropical North Pacific (ETNP), where denitrification plays an unequivocal role in N_2O production and consumption [*Yoshinari et al.*, 1997]. The high $\delta^{18}O$ and SP of N_2O observed in the ETNP suggest the importance of denitrification in the OMZ in the western North Pacific, which led to the development of models for evaluating the role of denitrification in the distribution of N_2O at Station KNOT (44°N, 155°W) (data are given by *Toyoda et al.* [2002]).

2. Samples and Analytical Methods

[4] Water samples were collected at 16°N, 107°W in the ETNP (May–June 2000, R/V *Revelle*). Samples for N_2O analysis were collected in 250-mL glass serum vials, preserved with $HgCl_2$, and sealed with butyl rubber stoppers. Dissolved N_2O was extracted by sparging the water samples [*Toyoda et al.*, 2002], and then separated from other sparged gases using a silicagel-packed pre-column (1/4 inch o.d.,

[1]Department of Environmental Science and Technology, Tokyo Institute of Technology, Yokohama, Japan.
[2]Solution Oriented Research for Science and Technology (SORST) Project, Japan Science and Technology Agency (JST), Kawaguchi, Saitama, Japan.
[3]Frontier Collaborative Research Center, Tokyo Institute of Technology, Yokohama, Japan.
[4]Department of Environmental Chemistry and Engineering, Tokyo Institute of Technology, Yokohama, Japan.
[5]Department of Geology and Geophysics, University of Hawaii, Honolulu, Hawaii, USA.
[6]Department of Oceanography, University of Hawaii, Honolulu, Hawaii, USA.
[7]Mutsu Institute for Oceanography, Japan Agency for Marine-Earth Science and Technology, Mutsu, Aomori, Japan.

0094-8276/05/2004GL021458$05.00

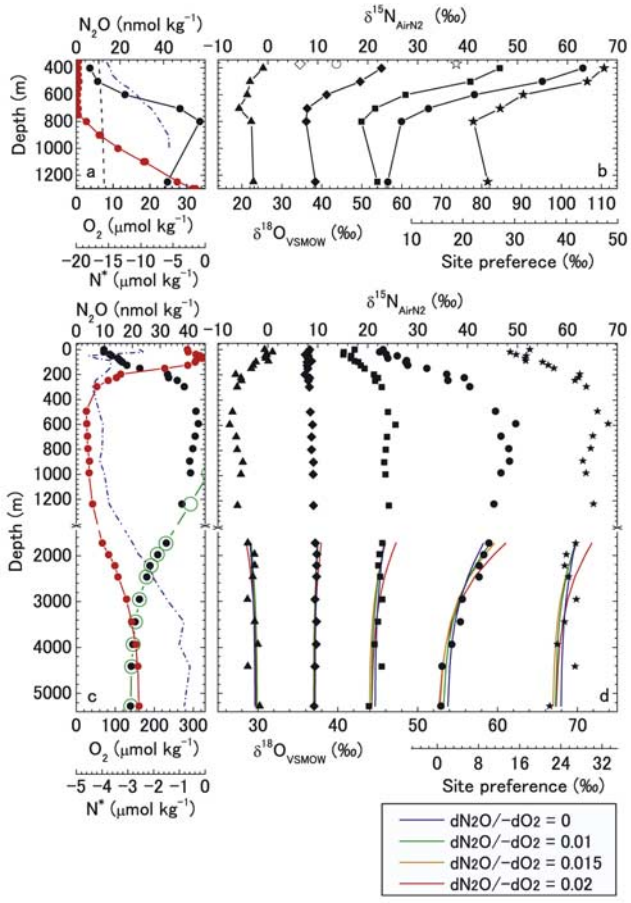

Figure 1. Vertical profiles of N_2O and O_2 concentrations, N*, and N_2O isotopomer ratios in the ETNP (a and b) and at Station KNOT (c and d). (a) and (c): N_2O concentration (filled black circle), O_2 concentration (filled red circle), and N* (blue dash-dotted line). (a): equilibrium N_2O concentration (broken line). (c): model I (green open circle; $dN_2O/-dO_2$ = 0.01 nmol/μmol). (b) and (d): $\delta^{15}N^{bulk}$ (filled diamond),$\delta^{15}N^{\alpha}$ (filled square), $\delta^{15}N^{\beta}$ (filled triangle), $\delta^{18}O$ (filled circle), and the site preference (filled star) of the dissolved N_2O. (b): $\delta^{15}N^{bulk}$ (open diamond), $\delta^{18}O$ (open circle), and site preference (open star) of the tropospheric N_2O [*Yoshida and Toyoda*, 2000]. (d): model II (see the legend.).

150-cm long s.s. tube, 60/80 mesh, 70°C) and a PoroPLOT-Q analytical column (0.32 mm i.d., df = 10 μm, 25 m, Chrompack, 27°C.) by gas chromatography [*Toyoda et al.*, 2005]. The concentration and isotopomer ratios of N_2O were measured by continuous-flow isotope-ratio monitoring mass spectrometry [*Yoshida and Toyoda*, 2000]. The analytical precisions for samples containing more than 20 nmol kg^{-1} N_2O were less than 1% (CV) for the concentration, and 0.2‰, 0.4‰, 0.6‰, 0.4‰, and 0.9‰ (1σ) for the $\delta^{15}N^{bulk}$, $\delta^{15}N^{\alpha}$, $\delta^{15}N^{\beta}$, $\delta^{18}O$, and SP, respectively.

3. Results and Discussion

[5] The measured and equilibrium concentrations of N_2O, its isotopomer ratios, O_2 concentration, and N* in the ETNP are shown in Figures 1a and 1b ($N^* \equiv [NO_3^-] - 16\,[PO_4^{3-}] +$ 2.90 μmol kg^{-1} [*Deutsch et al.*, 2001]). It is clear from the N* data that at oxygen levels below 1 μmol kg^{-1}, reduction of N_2O by denitrification is the dominant process at the depth of 400–750 m. Increases in $\delta^{15}N^{bulk}$ and $\delta^{18}O$ of the residual N_2O are due to the kinetic isotope effect of N_2O reduction by denitrification [*Yoshinari et al.*, 1997]. The data between 400 and 700 m in the ETNP (Figure 1b) indicate that the $\delta^{15}N^{\alpha}$ and SP also increase, whereas the $\delta^{15}N^{\beta}$ is nearly constant.

[6] The N_2O concentration maximum was located at 800 m (O_2 = 2.7 μmol kg^{-1}) in the ETNP, whereas the maximum is located at 500–600 m in the OMZ in the western North Pacific (see Figures 1a and 1c) [*Toyoda et al.*, 2002]. The $\delta^{15}N$, $\delta^{18}O$, and SP of N_2O at 595 m (27.1 μmol kg^{-1} O_2) at Station KNOT are 9.1‰, 62.3‰, and 33.2‰, respectively(data for 991013 are given by *Toyoda et al.* [2002]). The high values of $\delta^{18}O$ and SP of N_2O relative to those of the troposphere (see Figure 1b) observed at the concentration maxima are not consistent with those of N_2O produced by nitrification estimated at subsurface in the subtropical North Pacific gyre ($\delta^{15}N$ = 4 ± 1‰, $\delta^{18}O$ = 38.5 ± 3‰, and SP = 4 ± 4‰) [*Popp et al.*, 2002]. Thus, high $\delta^{18}O$ and SP are attributed to the N_2O reduction by denitrification. Considering oxygen levels higher than 1 μmol kg^{-1} at these maxima, N_2O production dominates over N_2O consumption [*Suntharalingam et al.*, 2000]. Thus, N_2O may be produced by nitrification, and also produced and consumed by denitrification.

[7] At Station KNOT, in situ denitrification in the OMZ is indicated by the observed negative N* (Figure 1c) and the possibility of nitrate consumption in the microzones of aggregates under aerobic conditions [*Wolgast et al.*, 1998]. *Li and Peng* [2002] suggested the possibility of N loss by denitrification in the equatorial Indian Ocean and the North Pacific based on the analysis of remineralization ratios. The profiles of N_2O concentration and isotopomer ratios suggest that the N_2O with high $\delta^{18}O$ and SP values is produced in the OMZ and then diffuses into aerobic waters above and below the OMZ, where the dissolved N_2O is characterized by the low $\delta^{18}O$ and SP values relative to those of the OMZ. The $\delta^{15}N^{bulk}$ of N_2O in the OMZ should be close to those in the surrounding aerobic waters.

[8] Considering that the waters between 1500 m and the bottom are homogeneous on the isopycnal surface along the longitude and latitude (see P1 and P13 of eWOCE in the work by *Schlitzer* [2000]), we developed one-dimensional, diffusion-advection models for the distribution of N_2O. Production ratio of N_2O during nitrification is constant at the oxygen levels above ~6 μmol kg^{-1} and increases drastically as the oxygen concentration decreases [*Jørgensen et al.*, 1984]. Thus, we assumed a constant ratio of N_2O production to O_2 consumption ($dN_2O/-dO_2$) during remineralization followed by nitrification in aerobic deep waters. Applying steady state conditions, we obtain equations for N_2O and O_2 concentrations as follows:

$$K\left(\partial^2 X/\partial z^2\right) - V(\partial X/\partial z) + cf(z) = 0, \quad (1)$$

$$K\left(\partial^2 O/\partial z^2\right) - V(\partial O/\partial z) - f(z) = 0, \quad (2)$$

where X and O are concentrations of N_2O and O_2, respectively, K is the eddy diffusion coefficient, V is the

advection velocity, c is a constant of $dN_2O/-dO_2$, and $f(z)$ is the consumption rate of O_2 as a function of depth z. Eliminating $f(z)$ in equations (1) and (2), and then integrating, the following equation (Model I: N_2O-O_2 model) is obtained:

$$X_z = -cO_z + C_1 + C_2 \exp(\omega z), \quad (3)$$

where the subscript z denotes in situ concentration, C_1 and C_2 are constants, and ω is V/K (-1.1×10^{-3} m^{-1}: estimation from salinity using the diffusion-advection model of *Munk* [1966]). Curve fitting of equation (3) to the observed data (991013 in the work by *Toyoda et al.* [2002]) estimates the $dN_2O/-dO_2$ value. The model can be applied only at the depths where $dN_2O/-dO_2$ is constant. Thus, we used the data at 5279 m (the maximum depth) for linking C_1 with C_2 to fix the deepest point of the model in the plots of N_2O vs. O_2, and then estimated the range of the depths, where the model can be applied, at 1729–5279 m using curve fitting. The constants c and C_1 were determined to minimize the least squares within the depths.

[9] We also estimated $dN_2O/-dO_2$ from the profiles of the N_2O isotopomer ratios using the isotopomer mass balance equations for mixing of three sources of N_2O. We first assumed that the dissolved N_2O primarily originated from the three types of N_2O: N_2O produced under suboxic conditions (denoted as N_2O_{subo}), N_2O produced by nitrification in aerobic deep waters (denoted as N_2O_{nit}), and N_2O confined to the bottom waters, which were formed from preindustrial surface waters (denoted as N_2O_{pre}) [*Bange and Andreae*, 1999]. The second assumption is that preindustrial surface waters were in equilibrium with the preindustrial troposphere and that the isotopomer ratios of N_2O_{pre} are equal to the ratios of the preindustrial tropospheric N_2O. Then, the isotopomer mass balance equation for each isotopomer is described as follows:

$$\delta_z X_z = \delta_{pre} X_{pre} + \delta_{nit} c\left(O_{pre} - O_z\right) + \delta_{subo}\{C_3 + C_2 \exp(\omega z)\}, \quad (4)$$

where X_{pre} and O_{pre} are N_2O_{pre} and O_{2pre}, namely the equilibrium concentrations of N_2O and O_2 in the preindustrial surface seawater, respectively, and δ_{pre}, δ_{nit}, and δ_{subo} are the N_2O isotopomer ratios of N_2O_{pre}, N_2O_{nit}, and N_2O_{subo}, respectively, and $C_3 = C_1 - X_{pre} - c\ O_{pre}$.

[10] The concentrations of N_2O_{pre} and O_{2pre} were estimated at 11.31 nmol kg^{-1} and 331.3 μmol kg^{-1}, respectively, by the equilibrium calculations [*Weiss and Price*, 1980; *Weiss*, 1970], with the following condition: N_2O in the preindustrial troposphere = 265 ppb [*Flückiger et al.*, 2002], potential temperature = 2°C, and salinity = 35‰ [*Bange and Andreae*, 1999]. The isotopomer ratios of the preindustrial tropospheric N_2O were estimated at 8.7‰ for $\delta^{15}N^{bulk}$, 45.8‰ for $\delta^{18}O$ [*Röckmann et al.*, 2003], and 19.1‰ for SP [cf. *Röckmann et al.*, 2003; *Yoshida and Toyoda*, 2000]. The concentration and isotopomer ratios of N_2O_{nit} are c (O_{pre} - O_z) μmol kg^{-1}; and 4.0‰ for $\delta^{15}N^{bulk}$, 38.5‰ for $\delta^{18}O_{VSMOW}$, and 4.0‰ for SP [*Popp et al.*, 2002]. Moreover, the concentration of N_2O_{subo} is given as: $C_3 + C_2 \exp(\omega z)$. We fitted the isotopomer ratios calculated by equation (4) to the observed ratios, and then determined the values of the $\delta^{15}N^{bulk}$, $\delta^{18}O$, and SP of N_2O_{subo} by fitting the model at every $dN_2O/-dO_2$ value (Model II: Three mixing model).

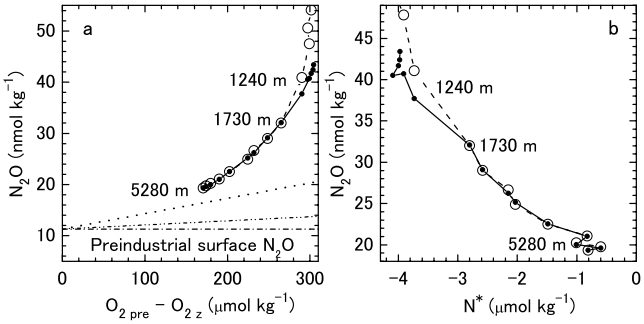

Figure 2. (a) Plots of N_2O concentration vs. the level of O_2 consumption (O_{pre}-O_z in equation (4)) and (b) plots of N_2O concentration vs. N* at Station KNOT. Each plot represents an observation (filled circle) and a model (open circle). The factors of the best fit models are as follows: (a) $dN_2O/-dO_2$ = 0.008 nmol/μmol (dashed double-dotted line), C_1 = 20.39 nmol kg^{-1}, C_2 = 81.28 nmol kg^{-1}, (b) dN_2O/dNO_3^- = 0.07 nmol/μmol, C_4 = 16.58 nmol kg^{-1}, and C_5 = 83.88 nmol kg^{-1}. (a): The range of $dN_2O/-dO_2$ is 0 (dash-dotted line) – 0.03 nmol/μmol (dotted line).

[11] Adopting the same procedure with model I, we obtain the correlation between N_2O and nitrate concentrations as follows (Model III: N_2O-nitrate model):

$$X_z = sN_z + C_4 + C_5 \exp(\omega z), \quad (5)$$

where s is the ratio of N_2O to nitrate production during nitrification in aerobic deep waters (dN_2O/dNO_3^-), N_z is the in situ nitrate concentration, and C_4 and C_5 are constants. Similar to Model I, we used the data at 5279 m for linking C_4 with C_5, and determined the constants s and C_4 by curve fitting to minimize the least squares at the depth of 1729–5279 m.

[12] The values of $dN_2O/-dO_2$ were estimated at 0.008 (0–0.03) and 0–0.015 nmol/μmol on the basis of models I (Figure 2a) and II (Figure 1d), respectively. The value of dN_2O/dNO_3^- was estimated at 0.07 (0–0.4) nmol/μmol on the basis of model III. Then, the N_2O concentrations of the model and the observations were plotted against N* (Figure 2b). The standard deviations of the errors of nonlinear least squares [*Laws*, 1997] were 0.22–0.26 nmol kg^{-1} N_2O (1σ, n = 9) within the range provided in parentheses, whereas the range obtained from model II was determined by the illustrated profiles. Our estimated values of $dN_2O/-dO_2$ are consistent with the ratio estimated by *Nevison et al.* [2003] for the South Atlantic and the South Indian Oceans (ΔN_2O/AOU = 0.01–0.05 nmol/μmol). Furthermore, our estimated values of dN_2O/dNO_3^- agree with the ratios estimated by the $^{15}NH_4$-added incubation experiments with the western North Pacific waters [*Yoshida et al.*, 1989] (dN_2O/dNO_3^- is 0.04–0.27 nmol/μmol at the depth of 0–2000 m). The ratio of $-dO_2/dNO_3^-$ estimated by the best fit results of Model I and III (0.07/0.008 = 8.8) is equal to the traditional Redfield ratio (138/16 = 8.6) [*Redfield*, 1958] within the range of errors, which indicates that the remineralization ratios can be the ratios of $P/N/C_{org}/-O_2/N_2O$ =

1/16/106/138/1.1 $\times 10^{-3}$ in the aerobic deep North Pacific (1729–5279 m at Station KNOT).

[13] Model I can estimate the contributions of the OMZ-originated N_2O ($C_3 + C_2 \exp(\omega z)$) and the aerobic nitrification ($c (O_{pre} - O_z)$) to the dissolved N_2O, for example 47.4 (41.3–54.5) % and 7.2 (0–13.5) %, respectively, at 2465 m at Station KNOT when $dN_2O/-dO_2$ is 0.008 (0–0.015) nmol/μmol (N_2O = 24.9 nmol kg^{-1} and $O_{2\,pre} - O_{2\,z}$ = 224.5 μmol kg^{-1} in Figure 2a.). The model indicates that diffusion of N_2O from the OMZ forms the correlation between ΔN_2O and AOU. The curvilinear relationship between ΔN_2O and AOU observed in the Pacific [*Cohen and Gordon*, 1979] is formed by upward advection as well as the increase of $dN_2O/-dO_2$, whereas the linear relationship in the Atlantic [*Yoshinari*, 1976] is attributed to the lack of advection ($\omega \approx 0$). The isotopomer ratios of the N_2O diffused from 1729 m to the bottom were estimated at 11.4 ± 1.0‰ for $\delta^{15}N^{bulk}$, 69.5 ± 4.5‰ for $\delta^{18}O_{VSMOW}$, and 34.5 ± 3.5‰ for SP using model II; hence the high $\delta^{18}O$ and SP of the diffused N_2O are useful tools for resolving the effect of diffusion on the N_2O distribution. Model III indicates that the anti-correlation between ΔN_2O and N* in aerobic waters is a result of mixing. In contrast, the N* minimum and N_2O concentration maximum in the OMZ should be the result of the in situ denitrification. Our models indicate that the N_2O production in the OMZ largely contributes to the oceanic N_2O distribution, whereas the nitrification in aerobic deep waters less contributes to the distribution.

[14] Our models do not fit data obtained from the depths shallower than 1238 m (41.3 μmol kg^{-1} O_2). The probable reasons are as follows: (1) a change in the diffusion coefficient of the main thermocline, (2) enhancement of N_2O production during nitrification under suboxic conditions, (3) N_2O production in the OMZ by denitrification, and (4) the effect of lateral diffusion. A combination of these factors might account for the disagreement.

[15] In conclusion, the increases of the $\delta^{18}O$-N_2O and SP in the OMZ are the signals of the N_2O consumption by denitrification. Thus, denitrification contributes to the N_2O production and consumption in the OMZ in the western North Pacific. Diffusion of the N_2O produced in the OMZ forms the correlation between ΔN_2O and AOU. Our models demonstrate that the denitrification hypothesis is consistent with the correlation between ΔN_2O and AOU, and the parallel ^{18}O-enrichment in N_2O and O_2 in the OMZ, which have been believed to be the evidence of the nitrification hypothesis.

[16] **Acknowledgments.** We thank T. M. Rust, and F. J. Sansone for sample collection, and oxygen and nutrients analyses in the ETNP. We wish to thank the crew of the R/V Revelle for their assistance on the cruise in the ETNP. We thank Y. Nojiri and N. Tsurushima for the cruise data including the oxygen and nutrients concentrations obtained from Station KNOT. We thank L. P. Gupta for discussing remineralization. This research was supported by NSF grants OCE 9810640 (BNP, FJS and Edward A. Laws) and OCE 0240787 (BNP). This is SOEST contribution number 6514.

References

Bange, H. W., and M. O. Andreae (1999), Nitrous oxide in the deep waters of the world's oceans, *Global Biogeochem. Cycles*, *13*(4), 1127–1135.

Cohen, Y., and L. I. Gordon (1979), Nitrous oxide production in the ocean, *J. Geophys. Res.*, *84*, 347–353.

Deutsch, C., A. Ganachaud, N. Gruber, R. M. Key, and J. L. Sarmiento (2001), Denitrification and N_2 fixation in the Pacific Ocean, *Global Biogeochem. Cycles*, *15*(2), 483–506.

Flückiger, J., E. Monnin, B. Stauffer, J. Schwander, T. F. Stocker, J. Chappellaz, D. Raynaud, and J.-M. Barnola (2002), High-resolution Holocene N_2O ice core record and its relationship with CH_4 and CO_2, *Global Biogeochem. Cycles*, *16*(1), 1010, doi:10.1029/2001GB001417.

Jørgensen, K. S., H. B. Jensen, and J. Sørensen (1984), Nitrous oxide reduction from nitrification and denitrification in marine sediment at low oxygen concentrations, *Can. J. Microbiol.*, *30*, 1073–1078.

Kim, K. R., and H. Craig (1990), Two-isotope characterization of N_2O in the Pacific Ocean and constraints on its origin in deep water, *Nature*, *347*, 58–61.

Laws, E. (1997), *Mathematical Methods for Oceanographers: An Introduction*, 343 pp., John Wiley, Hoboken, N. J.

Li, Y.-H., and T.-H. Peng (2002), Latitudinal change of remineralization ratios in the oceans and its implication for nutrient cycles, *Global Biogeochem. Cycles*, *16*(4), 1130, doi:10.1029/2001GB001828.

Munk, W. H. (1966), Abyssal recipes, *Deep Sea Res.*, *13*, 707–730.

Nevison, C., J. H. Butler, and J. W. Elkins (2003), Global distribution of N_2O and the ΔN_2O-AOU yield in the subsurface ocean, *Global Biogeochem. Cycles*, *17*(4), 1119, doi:10.1029/2003GB002068.

Popp, B. N., et al. (2002), Nitrogen and oxygen isotopomeric constraints on the origins and sea-to-air flux of N_2O in the oligotrophic subtropical North Pacific gyre, *Global Biogeochem. Cycles*, *16*(4), 1064, doi:10.1029/2001GB001806.

Redfield, A. C. (1958), The biological control of chemical factors in the environment, *Am. J. Sci.*, *46*, 205–221.

Röckmann, T., J. Kaiser, and C. A. M. Brenninkmeijer (2003), The isotopic fingerprint of the pre-industrial and the anthropogenic N_2O source, *Atmos. Chem. Phys.*, *3*, 315–323.

Schlitzer, R. (2000), Electronic atlas of WOCE hydrographic and tracer data now available, *Eos Trans. AGU*, *81*(5), 45.

Suntharalingam, P., and J. L. Sarmiento (2000), Factors governing the oceanic nitrous oxide distribution: Simulations with an ocean general circulation model, *Global Biogeochem. Cycles*, *14*(1), 429–454.

Suntharalingam, P., J. L. Sarmiento, and J. R. Toggweiler (2000), Global significance of nitrous-oxide production and transport from oceanic low-oxygen zones: A modeling study, *Global Biogeochem. Cycles*, *14*(4), 1353–1370.

Toyoda, S., and N. Yoshida (1999), Determination of nitrogen isotopomers of nitrous oxide on a modified isotope ratio mass spectrometer, *Anal. Chem.*, *71*(20), 4711–4718.

Toyoda, S., N. Yoshida, T. Miwa, Y. Matsui, H. Yamagishi, U. Tsunogai, Y. Nojiri, and N. Tsurushima (2002), Production mechanism and global budget of N_2O inferred from its isotopomers in the western North Pacific, *Geophys. Res. Lett.*, *29*(3), 1037, doi:10.1029/2001GL014311.

Toyoda, S., et al. (2005), Fractionation of N_2O isotopomers during production by denitrifier, *Soil Biol. Biochem.*, in press.

Weiss, R. F. (1970), The solubility of nitrogen, oxygen and argon in water and seawater, *Deep Sea Res.*, *17*, 721–735.

Weiss, R. F., and B. A. Price (1980), Nitrous oxide solubility in water and seawater, *Mar. Chem.*, *8*, 347–359.

Wolgast, D. M., A. F. Carlucci, and J. E. Bauer (1998), Nitrate respiration associated with detrital aggregates in aerobic bottom waters of the abyssal NE Pacific, *Deep Sea Res., Part II*, *45*, 881–892.

Yoshida, N., and S. Toyoda (2000), Constraining the atmospheric N_2O budget from intramolecular site preference in N_2O isotopomers, *Nature*, *405*, 330–334.

Yoshida, N., H. Morimoto, M. Hirano, I. Koike, S. Matsuo, E. Wada, T. Saino, and A. Hattori (1989), Nitrification rates and ^{15}N abundances of N_2O and NO_3^- in the western North Pacific, *Nature*, *342*, 895–897.

Yoshinari, T. (1976), Nitrous oxide in the sea, *Mar. Chem.*, *4*, 189–202.

Yoshinari, T., M. A. Altabet, S. W. A. Naqvi, L. Codispoti, A. Jayakumar, M. Kuhland, and A. Devol (1997), Nitrogen and oxygen isotopic composition of N_2O from suboxic waters of the eastern tropical North Pacific and the Arabian Sea—Measurement by continuous-flow isotope-ratio monitoring, *Mar. Chem.*, *56*(3–4), 253–264.

B. N. Popp, Department of Geology and Geophysics, University of Hawaii, Honolulu, HI 96817, USA.

H. Yamagishi and N. Yoshida, Department of Environmental Science and Technology, Tokyo Institute of Technology, 4259 Nagatsuta, Midori-ku, Yokohama, 226-8502 Japan. (hyamagishi@depe.titech.ac.jp)

S. Toyoda, Department of Environmental Chemistry and Engineering, Tokyo Institute of Technology, 4259 Nagatsuta, Midori-ku, Yokohama, 226-8502 Japan.

S. Watanabe, Mutsu Institute for Oceanography, Japan Agency for Marine-Earth Science and Technology, 690 Kitasekine, Sekine, Mutsu 035-0022, Aomori, Japan.

M. B. Westley, Department of Oceanography, University of Hawaii, Honolulu, HI 96817, USA.